Recovery of nanomolecular electronic states from tunneling spectroscopy: LDOS of low-dimensional phthalocyanine molecular structures on Cu(111)



2013 Nanotechnology 24 395704

(http://iopscience.iop.org/0957-4484/24/39/395704)

Nanotechnology **24** (2013) 395704 (11pp) doi:10.1088/0957-4484/24/39/395704

# Recovery of nanomolecular electronic states from tunneling spectroscopy: LDOS of low-dimensional phthalocyanine molecular structures on Cu(111)

**Y Yamagishi, S Nakashima, K Oiso and T K Yamada**

Graduate School of Advanced Integration Science, Chiba University, 1-33, Yayoi-cho, Inage-ku, Chiba-shi 263-8522, Chiba, Japan

E-mail: toyoyamada@faculty.chiba-u.jp

Received 14 May 2013, in final form 6 August 2013
Published 5 September 2013
Online at stacks.iop.org/Nano/24/395704

**Abstract**
Organic nanomolecules have become one of the most attractive materials for new nanoelectronics devices. Understanding of the electronic density of states around the Fermi energy of low-dimensional molecules is crucial in designing the electronic properties of molecular devices. The low dimensionality of nanomolecules results in new electronic properties owing to their unique symmetry. Scanning tunneling spectroscopy is one of the most effective techniques for studying the electronic states of nanomolecules, particularly near the Fermi energy ($\pm$1.5 eV), whereas these molecular electronic states are frequently buried by the tunneling probability background in tunneling spectroscopy, resulting in incorrect determination of the molecular electronic states. Here, we demonstrate how to recover nanomolecular electronic states from d$I$/d$V$ curves obtained by tunneling spectroscopy. Precise local density of states (LDOS) peaks for low-dimensional nanostructures (monolayer ultrathin films, one-dimensional chains, and single molecules) of phthalocyanine ($H_2Pc$) molecules grown on noble fcc-Cu(111) were obtained.

(Some figures may appear in colour only in the online journal)

## 1. Introduction

Organic molecules have enabled the realization of cheap, flexible, and printed electronic devices, which are nowadays widely used for organic solar cells [1], organic electroluminescence devices [2], organic displays [3], and organic light-emitting diodes [4]. So far, organic molecular films with a thickness of 10–100 nm grown on a substrate have been used, and electron or hole transfer through molecular junctions has determined the electronic properties of devices. Minimization of the device size is an important challenge for near-future electronics to realize low-cost devices with low power consumption and high functionality, which is why studies on nanoelectronics and nanoscience have rapidly developed in the last decade. Fundamental studies on nanomolecules of size 1–10 nm have recently been carried out and new electronic (spin) properties have been exhibited by single molecules [5–11], single-molecular chains [12], and monolayer (ML) molecular films [13, 14] on metal substrates. In particular, the local density of states of nanomolecules varies greatly owing to their unique symmetry, i.e., surface or interface effects mainly determine the nanodevice properties [5, 15]. Precise LDOS measurements of low-dimensional molecular structures (single molecules, one-dimensional (1D) molecular chains, and ultrathin films) are expected to open a new pathway toward nanoscale organic molecular electronics. A molecular film with a thickness of 10–100 nm has the highest occupied molecular orbital (HOMO) and lowest unoccupied molecular orbital (LUMO) states, which are known as bulk states. The bulk states will change when the film thickness is decreased to 1–10 nm. Such

 

films are usually treated as interfaces and it is well known that interfaces have different electronic states. However, so far the electronic states and molecular orbitals at interfaces have not been studied in depth, since present molecular devices use bulk states and the interface effect is a minor problem. However, at the scale of nanomolecules (of size 1–10 nm), interface or surface effects become a major issue since they will determine the electronic properties of near-future nanomolecular electronic devices.

One of the most effective techniques for precisely measuring the LDOS of 1-nm-size molecules is tunneling spectroscopy with a scanning tunneling microscopy (STM) setup, known as scanning tunneling spectroscopy (STS). This technique measures the so-called $I(V)$ curves or $\mathrm{d}I/\mathrm{d}V$ curves, which are the tunneling conductivity and differential tunneling conductivity as functions of the sample bias voltage, respectively. The bias voltage $V_S = 0$ corresponds to the Fermi energy, negative ($V_S < 0$) and positive ($V_S > 0$) voltages indicate energies below and above the Fermi energy, respectively. Since the $\mathrm{d}I/\mathrm{d}V$ curves are a convolution of the surface LDOS and the tunneling probability function ($T$ background) [16], the LDOS can be obtained by the normalization of $\mathrm{d}I/\mathrm{d}V$ curves using the $T$ background, i.e., $(\mathrm{d}I/\mathrm{d}V)/T$ below the Fermi energy ($V_S < 0$) indicates the occupied LDOS (HOMO) and $(\mathrm{d}I/\mathrm{d}V)/T$ above the Fermi energy ($V_S > 0$) indicates the unoccupied LDOS (LUMO) [15–18]. However, owing to the time-consuming nature of this normalization, $\mathrm{d}I/\mathrm{d}V$ or even $I(V)$ curves have mainly been used to study the LDOS. For metal surfaces with strong and sharp surface-state peaks, it is possible to study the LDOS without the above normalization [22, 25], but for samples with a broad, weak, or complicated LDOS near the Fermi energy, it is impossible to recover precise LDOS peaks (for example, [18]).

So far, molecules have been used as semiconductor materials in electronic devices, and therefore the HOMO and LUMO states are the most important key parameters determining the electronic properties. The LDOS near the Fermi energy has not been focused on since it lies inside the gap. However, it has recently been found that nanomolecules, especially $\pi$-conjugated single phthalocyanine molecules, on metal surfaces have metal-like properties (a large conductivity even at the Fermi energy as well as a magnetoresistance effect) [5–8], which is expected to open a new pathway toward using nanomolecules as new conductive and magnetic materials. The electronic properties of 1-nm-size single molecules are strongly affected by the electronic states of the substrate electrode, which shift the HOMO/LUMO states of the molecules and are likely to close the band gap and switch the electronic properties from semiconductor-like to metallic properties. Therefore, obtaining a better understanding of the LDOS near the Fermi energy of nanomolecules on metal substrates is now very important for the development of next generation nanomolecular electronics.

In this paper, we show that a normalization technique using a correlated fitted tunneling probability function ($T^{\mathrm{c}}_{\mathrm{fit}}$) is a powerful technique for recovering nanomolecular electronic states from $\mathrm{d}I/\mathrm{d}V$ curves obtained by tunneling spectroscopy. This normalization method is described in details. $(\mathrm{d}I/\mathrm{d}V)/T^{\mathrm{c}}_{\mathrm{fit}}$ curves obtained for low-dimensional phthalocyanine ($H_2Pc$) molecules (monolayer films, one-dimensional chains, and single molecules) on Cu(111) successfully recovered the molecular LDOS (HOMO and LUMO) peaks near the Fermi energy ($\pm$1.5 eV), which shows that $H_2Pc$ nanomolecules have metallic properties (i.e., no band gap).

## 2. Experimental details

Scanning tunneling microscopy (STM) and spectroscopy (STS) experiments were performed at 4.6 and 300 K in ultrahigh vacuum (UHV, base pressure $<8 \times 10^{-9}$ Pa). STS measurements were performed by opening the feedback loop of the tunneling current, i.e., fixing the tip–sample separation ($z$). The tunneling current was measured at each pixel by varying the sample voltage within $\pm$1.5 V to obtain $I(V)$ curves. In the case of metal surfaces, it has been reported that $\mathrm{d}I/\mathrm{d}V$ curves up to $\pm$3 V are required for normalization [17, 18]. However, in the case of molecular surfaces, higher voltages may damage the molecules. Thus, we only apply a bias up to 1.5 V. Differential conductivity ($\mathrm{d}I/\mathrm{d}V$) curves were obtained by numerical differentiation of the $I(V)$ curves. Although a lock-in amplifier was used to obtain the $\mathrm{d}I/\mathrm{d}V$ signals in our previous papers [5, 7], here we do not use a lock-in amplifier so that we can distinguish between real and pseudogaps around the Fermi energy.

Tungsten (W) tips were used as STM tips, which were electrochemically etched from W wires ($\phi = 0.3$ mm, purity 99.9%) in air using KOH aq., while the etching process was monitored by optical microscopy. Subsequently, the tip was rinsed with hot water and acetone, then transferred into the load lock chamber of our STM setup. The apex of the W tip was sputtered with $Ar^+$ in UHV and annealed at temperatures of up to 2000 K to obtain a clean apex.

Cu(111) and Ag(001) single crystals (purity 99.999%) were used as conductive substrates. A clean and atomically flat surface was obtained after several sputtering and annealing cycles in UHV. Phthalocyanine ($H_2Pc$) molecules were used. Commercial $H_2Pc$ powder (Alfa Aesar, purity 95%) was purified by sublimation at 653 K and recrystallization at 473 K at a pressure of $10^{-3}$ Pa (yield 30%). Nuclear magnetic resonance (NMR) and infrared spectra confirmed the absence of impurities after the purification. The clean $H_2Pc$ powder was placed in a crucible, which was set in a molecular chamber and heated to 550 K. The $H_2Pc$ powder was deposited on the clean Cu(111) single crystals at 300 K by opening the shutter valve between the preparation and molecular chambers. The deposition rate on Cu(111) was 0.03 ML $\mathrm{min}^{-1}$, calibrated by STM images.

## 3. Results and discussions

Organic molecules are now widely used as semiconductor materials for electronic devices. Minimization of the devices is one of the key issues in realizing high functionality, low cost, and low power consumption. Recently, nanomolecules

(single molecules, chains of molecules, and ultrathin films) [5–14] on metal substrates have been found to exhibit new electronic properties, such as metallic high conductivity and magnetoresistance effect [5, 6]. The origin of these new electronic properties is a previously undiscovered electronic interface state generated by electronic coupling between the molecular orbitals and the metal LDOS. Such 1-nm-size ultrasmall molecules on a metal substrate are likely to exhibit new electronic properties instead of those intrinsic to semiconductor molecules. The electronic properties are dependent on the LDOS near the Fermi energy (HOMO/LUMO). Precise understanding of the LDOS around the Fermi energy is the key to realizing new nanomolecular conductive electronic (spintronic) devices. Tunneling spectroscopy with an STM setup is one of the most effective methods of precisely obtaining the LDOS of nanomolecules on metal substrates. However, the results obtained from tunneling spectroscopy include not only the LDOS but also the $T$ background. The observed $\mathrm{d}I/\mathrm{d}V$ characteristics greatly vary with the $T$ background, which frequently results in incorrect values of the LDOS. Here, we show how to recover LDOS peaks from the $\mathrm{d}I/\mathrm{d}V$ curves by normalization using $T^{\mathrm{c}}_{\mathrm{fit}}$.

First, we explain a tunneling spectroscopy. The tunneling current ($I$) is plotted as a function of the sample bias voltage ($V_{\mathrm{S}}$) under constant tip–sample separation ($z$), which gives the so-called $I(V)$ (nA) curves. Then, numerical differentiation gives the differential conductivity $\mathrm{d}I/\mathrm{d}V$ (nA $\mathrm{V}^{-1}$) curves, which correspond to the product of the LDOS and the tunneling probability function ($T$) within the WKB approximation [16–18];

$$(\mathrm{d}I/\mathrm{d}V)/T \propto \mathrm{LDOS}, \tag{1}$$

$$T = T^{+} + T^{-}, \tag{2}$$

$$T^{+} = a^{+} \exp\left[-b\sqrt{\phi - V_{\mathrm{S}}/2}\right], \tag{3}$$

$$T^{-} = a^{-} \exp\left[-b\sqrt{\phi + V_{\mathrm{S}}/2}\right], \tag{4}$$

where $b = 2\sqrt{2m/\hbar^2}z \simeq 1.02z$ ($m$: electron mass, $\hbar$: Planck's constant/$2\pi$, $V_{\mathrm{S}}$: sample bias voltage) and the dimension of $z$ is Å. $\phi$ denotes the averaged work function of the tip and sample, which is typically from 3 to 6 eV. $a^{+}$ and $a^{-}$ are proportionality coefficients for positive and negative voltages, respectively. Negative and positive voltages indicate occupied and unoccupied density of states, respectively.

Figure 1(a) shows simulated LDOS (solid line) peaks and tunneling probability functions ($T$, dotted lines). The convolution of the LDOS(1) and $T(1)$ curves is the $\mathrm{d}I/\mathrm{d}V(1)$ curve shown in figure 1(b), in which a peak can still be observed. Note that the LDOS detected by STM is that at the apex of the tip (i.e., LDOS of the sample in vacuum, 0.5–1.0 nm above the surface). The LDOS decays with increasing $z$. Also, $T$ changes with $z$. Therefore, at different tip–sample separations ((1) $z = 9$ Å, (2) $z = 10$ Å, (3) $z =$ 11 Å in figure 1) [1], we obtain different $\mathrm{d}I/\mathrm{d}V$ curves even on the same sample surface as shown in figure 1(b).

$\mathrm{d}I/\mathrm{d}V$ measurements have led to the discovery of many surface states on metal surfaces including Cu(111) [20], Au(111) [21], Fe(001) [22, 23], Co(0001) [24], Mn(001) [17, 18], and Cr(001) [25]. These spectroscopy measurements on metal surfaces are typically performed at a tunneling resistance of $R = 10^{9}$–$10^{10}$ Ω (e.g. $V_{\mathrm{S}} = 1$ V, $I = 0.1$–$1.0$ nA). However, on molecular surfaces, care should be taken when performing tunneling spectroscopy measurements.

Figures 1(c) and (d) show an example how $H_2Pc$ molecular structures are modified during STM measurements. Here, we deposited about 0.3 ML $H_2Pc$ molecules on a Ag(001) surface at 300 K. The molecules diffuse on the surface and accumulate at the steps, resulting in step-flow growth. Molecules are observed as bright spots in these figures. We scanned the same area several times using the STM tip with $R = 2 \times 10^{10}$ Ω. Figures 1(c) and (d) show STM images taken before and after the scan, respectively. It is clear that now the molecular structures change as a result of scanning (see the arrows in figures 1(c) and (d)). When $R = 10^{9}$–$10^{10}$ Ω, strong tip–sample interactions appear, which are likely to modify the molecular structures during each scan. This is not ideal for obtaining stable and reproducible tunneling spectra since $z$ must be constant during the tunneling spectroscopy measurement (i.e., opened feedback loop).

A simple means of reducing the strong tip–sample interaction is to increase the tunneling resistance, i.e., by increasing the value of $z$, although a large value of $z$ markedly decreases the value of $T$. Also, the LDOS on the molecular surface rapidly decays in vacuum, resulting in a weak $\mathrm{d}I/\mathrm{d}V$ signal.

In figure 1(b), we have shown how the value of $z$ affects $\mathrm{d}I/\mathrm{d}V$. Although an LDOS peak can be clearly observed in the $\mathrm{d}I/\mathrm{d}V(1)$ curve, it is difficult to observe details of the molecular electronic orbital states in the $\mathrm{d}I/\mathrm{d}V(3)$ curve. This might lead to an incorrect conclusion, for example, that there is a gap around the Fermi energy. The result of this simple simulation indicates that $\mathrm{d}I/\mathrm{d}V$ measurements on molecular surfaces are more difficult than those on metal surfaces. For tunneling spectroscopy measurement at a tunneling resistance larger than $10^{10}$ Ω, a good signal-to-noise ratio (S/N) is necessary to detect small signals in $I(V)$ curves and normalization using $T$ is necessary to precisely recover the molecular LDOS (HOMO/LUMO).

A large tunneling resistance ($R$) can be obtained by increasing the tip–sample separation. However, on molecular surfaces, maximum voltage set to 1.5 V should be applied to avoid damage. Also, a typical commercial scanning tunneling microscope has a current noise of 5–20 pA. These facts prevent $I(V)$ measurements at a large tunneling resistance, for example, $R = 1 \times 10^{11}$ Ω with $V_{\mathrm{S}} = 1$ V and $I =$ 10 pA. To perform $I(V)$ measurements on molecular surfaces, low-current-noise is necessary. We used a low-current-noise amplifier and cables with a low capacitance (50 pF $\mathrm{m}^{-1}$),

[1] A tip–sample separation ($z$) is zero when the tip contacts to the sample [19], where the resistance is approximately $10^{4}$ Ω. As $R \propto V\exp(2\kappa z)$, at $R = 10^{9}$ Ω, $z$ is estimated to be about 0.8–0.9 nm.

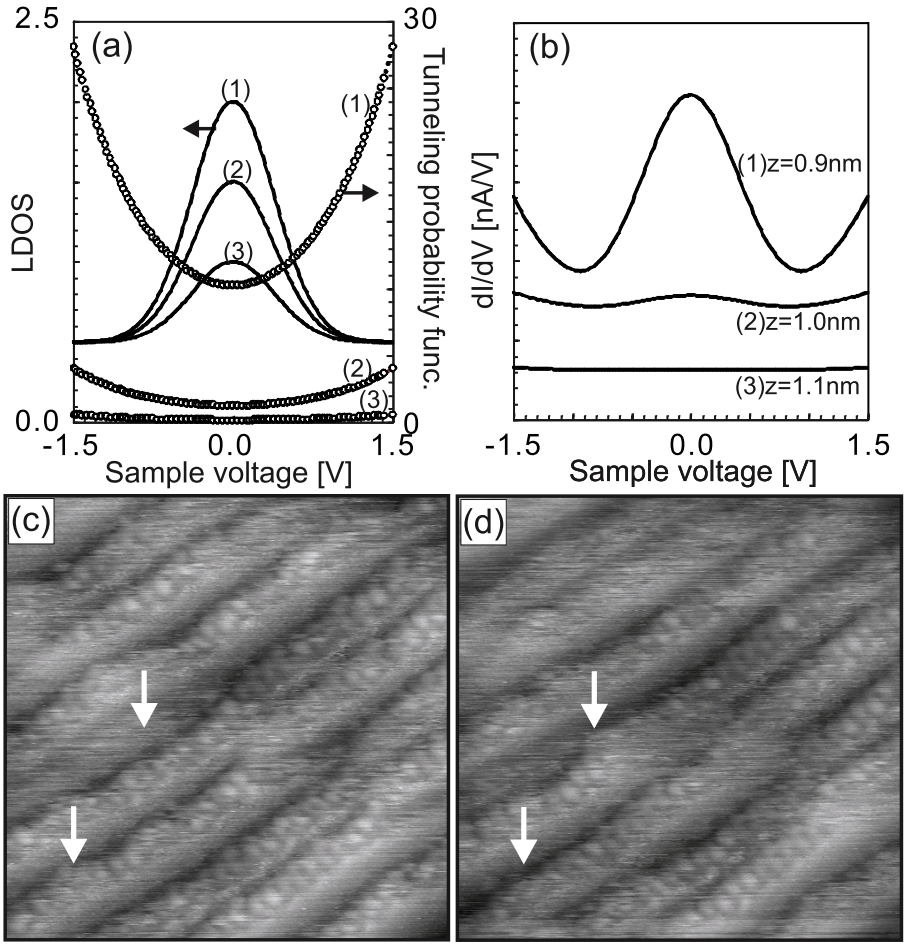


**Figure 1.** (a) Simulated LDOS peaks (solid lines) and tunneling probability functions ($T$: open circles). LDOS peaks are simulated by Gaussian functions, whose peak amplitudes are 1.5, 1.0, and 0.5 for (1), (2), and (3), respectively. Tunneling probability functions are simulated with a constant averaged barrier height ($\phi$) of 4.5 eV with different tip–sample separations ($z$) of 9, 10, and 11 Å for (1), (2), and (3), respectively. (b) Simulated d$I$/d$V$ curves with $T$ and LDOS peaks in (a). (c) and (d) show STM topographic images obtained at the same surface of 0.3 ML $H_2Pc$ on stepped Ag(001) ($20 \times 20$ nm$^2$, $V_s = -1300$ mV, $I = 50$ pA). Single molecules (bright spots) accumulate at atomic steps. Before and after ((c) and (d)) scanning the same area with an STM tip, the molecular structures changed, which are marked by arrows.

which markedly decreased the base current noise to $\sim 5$ fA Hz$^{-1/2}$ (see figure 2(a)), whereas noise remained at 100 Hz (15 fA Hz$^{-1/2}$).

Test spectroscopy measurements were first performed at a large tunneling resistance (up to $R = 2 \times 10^{11}$ Ω) on a Cu(111) surface. A clean and atomically flat Cu(111) surface prepared by several cycles of sputtering and annealing is shown in figure 2(b-1). The atomic steps follow the hexagonal symmetry of fcc(111). The terrace widths are typically 50–100 nm. Figures 2(b-2) and (b-3) show a low energy electron diffraction pattern and an atomically resolved STM image obtained on this surface, respectively. Figure 2(c) shows an $I(V)$ curve obtained at $R = 1 \times 10^{11}$ Ω by averaging 100 single curves to reduce statistical errors. The $I(V)$ curve was numerically differentiated and normalized using its fitted $T$. Figure 2(d) shows the recovered surface-state peak of Cu(111) at different tunneling resistances of $1 \times 10^{10}$, $3 \times 10^{10}$, $1 \times 10^{11}$, and $2 \times 10^{11}$ Ω. In all cases, the (d$I$/d$V$)/$T$ curves successfully recovered the occupied LDOS peak at approximately −150 meV. We consider that the S/N ratio of the current is sufficiently high to perform d$I$/d$V$ measurements at large tunneling resistances of $10^{10}$–$10^{11}$ Ω on molecular surfaces.

To evaluate how well the $T$ normalization technique recovers molecular surface states, we used $H_2Pc$ nanomolecular structures (ultrathin films, 1D chains, and single molecules) on Cu(111). $H_2Pc$ molecules have been widely used for fundamental research [5–8] as well as in molecular electronics [1]. The Cu(111) substrate is also a typical fcc close-packed noble metal surface, whose electronic structure has been studied in detail [20].

Figure 3 shows STM results obtained on Cu(111) surfaces with ((a), (b)) 0.7 ML and ((c), (d)) 1.5 ML $H_2Pc$ molecules. As shown in figure 3(a), single molecules were found adhering to the Cu(111) surface along three different directions: −15°, +15°, and +45° from the [$\bar{1}$10] direction of fcc-Cu(111), i.e., molecules have stable sites of A, B, and C along directions with intervals of 30°. Figure 3(b) shows a model of $H_2Pc$ molecules on a Cu(111) surface, assuming the

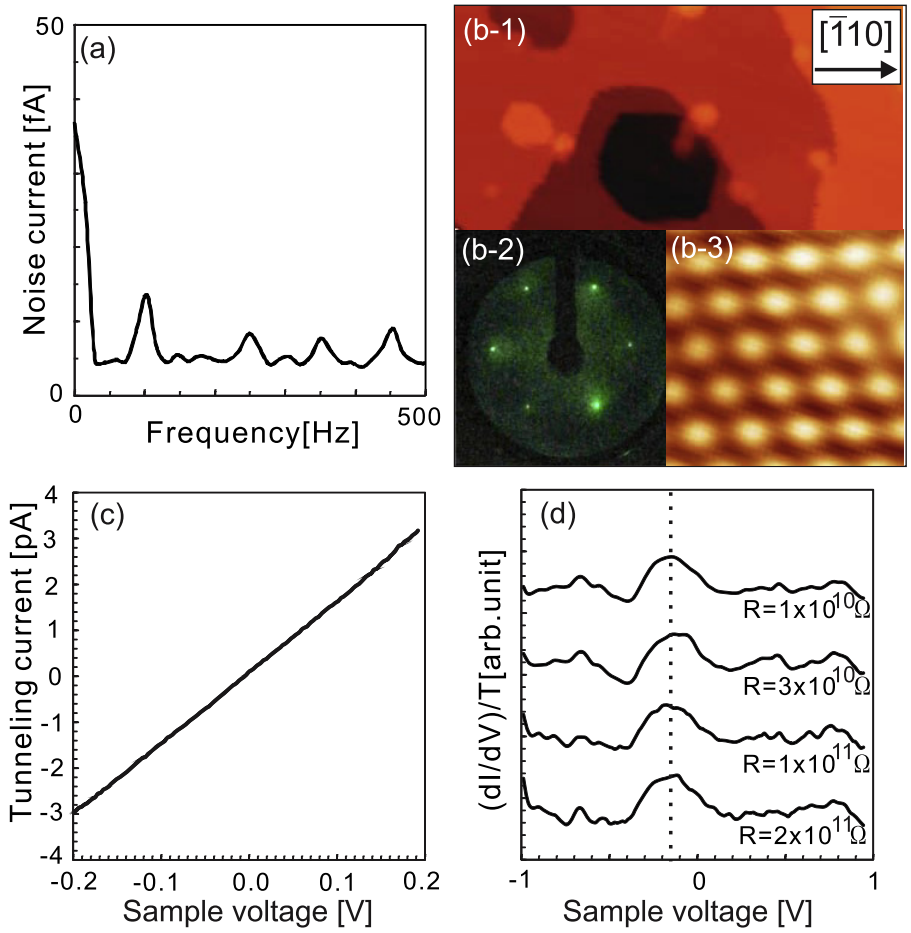


**Figure 2.** All measurements were performed on a clean and atomically flat fcc-Cu(111) surface. (a) Noise spectrum of tunneling current of our STM setup. (b-1) shows an STM topographic image (150 × 75 nm$^2$, $V_s = -2$ V, $I = 50$ pA). Several terraces are observed. (b-2) A low energy electron diffraction pattern with a kinetic energy of 113 eV. (b-3) An atomically resolved STM image (1.5 × 1.5 nm$^2$, $V_s = -2$ mV, $I = 2$ nA). (c) An $I(V)$ curve averaging 100 single curves at $R = 6 \times 10^{10}$ Ω. (d) Normalized $(dI/dV)/T$ curves correspond to LDOS at different tunneling resistances of $R = 1 \times 10^{10}$, $3 \times 10^{10}$, $1 \times 10^{11}$, and $2 \times 10^{11}$ Ω.

atoms to be spherical. 36, 30, and 25% of the single molecules adhered on the surface at sites A, B, and C, respectively.

Figures 3(c)–(e) show STM topographic images obtained on the surface of 1.5 ML $H_2Pc$ molecules on Cu(111). Molecules grew in a layer-by-layer mode (figure 3(c)) and formed a densely packed tetragonal lattice structure. Three different domains were observed with alignments corresponding to site A, B, and C of single molecules as shown in figures 3(d) and (e).

We performed tunneling spectroscopy measurements on this densely packed film surface. Since the molecular film has a higher stability than single molecules and molecular chains, we obtained stable tunneling spectra at $R = 1 \times 10^{10}$–$2 \times 10^{11}$ Ω and even at 300 K. An experimentally obtained $dI/dV$ curve (dotted line) is shown in figure 4(a). Owing to the large $R$, the obtained $dI/dV$ value at −1.5 V (0.05–0.10 nA V$^{-1}$) is much smaller than $dI/dV$ values measured on metal surfaces at −1.5 V (typically 5–10 nA V$^{-1}$) [17, 18]. Shoulders and bumps are observed near the Fermi energy, which indicate molecular LDOS peaks. Although $T$ normalization can recover the peaks, it should first be determined whether there is a gap at the Fermi energy. If a $dI/dV$ curve with a gap is normalized by $T$, a pseudopeak can appear in the $(dI/dV)/T$ curve. The $dI/dV$ curve in figure 4(a) has a value of 0.003 nA V$^{-1}$ at the Fermi energy ($V_S = 0$), which means that the first $H_2Pc$ layer on Cu(111) has no gap, i.e. it exhibits a metallic property. We can now normalize the $dI/dV$ curve using $T$ to recover the molecular LDOS.

An important point in the normalization is how to obtain the $T$ background from the experimentally obtained $dI/dV$ curve. $T$ normalization on metal surfaces is carried out as follows [17, 18]. At higher voltages, the main contribution to $dI/dV$ is the exponential $T$ background instead of LDOS signals, which means that $T$ can be easily obtained by fitting to $dI/dV$ values at high voltages. $dI/dV$ curves are measured up to ±3 V. $T_+$ (equation (3)) is obtained by fitting to the $dI/dV$ values in the range of +2.5–+3.0 V. The average work function $\phi$ was assumed to be about 4 eV. The two parameters $a^+$ and $b$ are obtained. In the same way, $T^-$ (equation (4)) is fitted to $dI/dV$ values in the range of −2.5 to −3.0 V, and $a^-$ is obtained. Finally, from the fact that $T = T^+ + T^-$ (equation (2)), the experimentally obtained $dI/dV$ curve is normalized. A $(dI/dV)/T$ curve (equation (1)) is proportional to the LDOS.

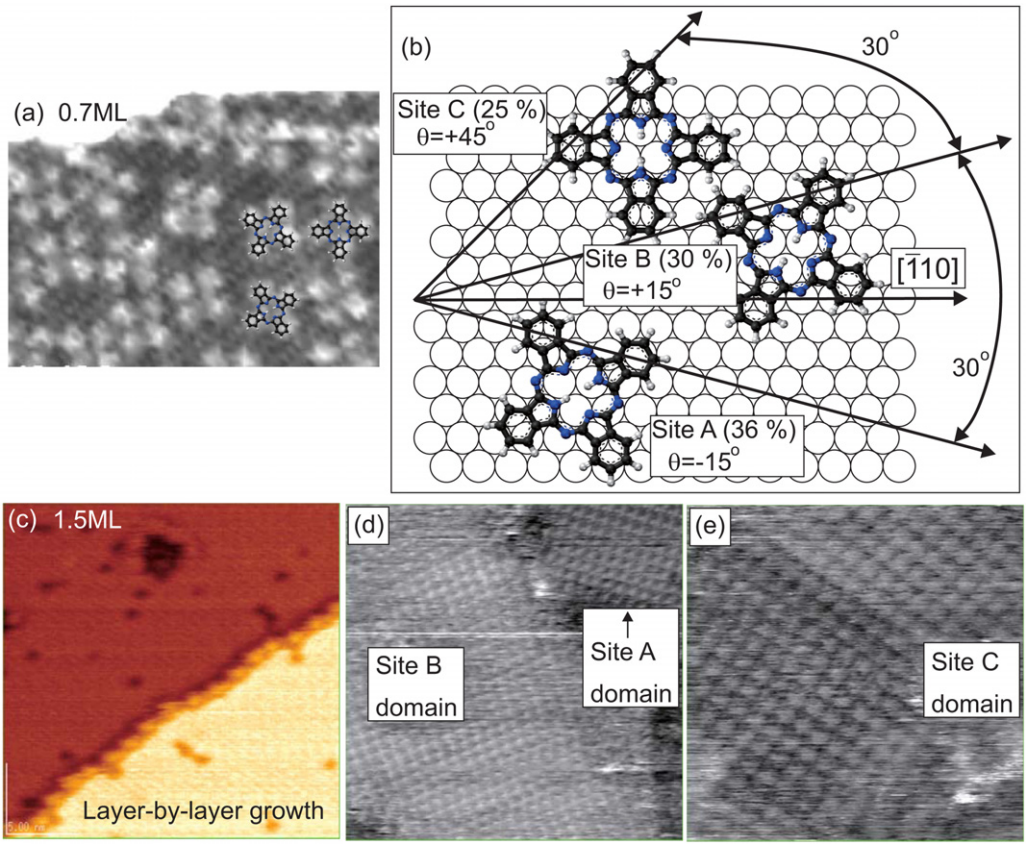


**Figure 3.** (a) An STM topographic image obtained on 0.7 ML $H_2Pc$ on Cu(111) at 4.6 K ($14 \times 10$ nm$^2$). Single $H_2Pc$ molecules are observed. (b) A model of single $H_2Pc$ molecules on a fcc-Cu(111) surface. Spheres reveal atoms. Three absorption sites were observed. (c)–(e) show STM topographic images obtained on 1.5 ML $H_2Pc$ on Cu(111) at 300 K ($20 \times 20$ nm$^2$ for (c) and (e), $30 \times 30$ nm$^2$ for (d)). First and second layers are observed. Three different domains were observed, which alignments correspond to site A, B, and C of single molecules.

However, on molecular surfaces, it is difficult to measure the tunneling spectra at high voltages which damage the molecules (e.g., figures 1(c) and (d)). In this study, we were able to measure reliable tunneling spectra up to $\pm 1.5$ V while keeping the tunneling resistance larger than $R = 1 \times 10^{10}$ Ω (e.g. as indicated in figure 4(a), there was no damage to $H_2Pc$ molecules after the measurements, whereas an applied voltage of more than 2.5 V damaged the molecules even at $R = 10^{11}$ Ω).

In this study, $T^+$ in equation (3) was fitted to $\mathrm{d}I/\mathrm{d}V$ values in the range of $+1.0$–$+1.5$ V, and $T^+_{\mathrm{fit}}$ in figure 4(a) (thin black line) was obtained. $T^-$ in equation (4) was fitted to $\mathrm{d}I/\mathrm{d}V$ values in the range of $-1.0$ to $-1.5$ V, and $T^-_{\mathrm{fit}}$ in figure 4(a) (thin gray line) was obtained. Note that the shape of the $\mathrm{d}I/\mathrm{d}V$ curve in figure 4(a) above $+1$ V and below $-1$ V appears to be linear rather than exponential. Therefore, $T_{\mathrm{fit}} = T^+_{\mathrm{fit}} + T^-_{\mathrm{fit}}$ frequently becomes larger than the experimentally obtained $\mathrm{d}I/\mathrm{d}V$ around the Fermi energy ($T_{\mathrm{fit}} > \mathrm{d}I/\mathrm{d}V$). However, in principle, the $T$ background must be smaller than $\mathrm{d}I/\mathrm{d}V$. Therefore, we need to correlate $T_{\mathrm{fit}}$ by introducing an offset $c$ (nA V$^{-1}$),

$$(\mathrm{d}I/\mathrm{d}V)/T^{\mathrm{c}}_{\mathrm{fit}} \propto \mathrm{LDOS}, \tag{5}$$

$$T^{\mathrm{c}}_{\mathrm{fit}} = T^+_{\mathrm{fit}} + T^-_{\mathrm{fit}} - c > 0, \tag{6}$$

$$c = T(V_{\mathrm{S}} = 0) - \mathrm{d}I/\mathrm{d}V(V_{\mathrm{S}} = 0). \tag{7}$$

We normalized $\mathrm{d}I/\mathrm{d}V$ using the corrected fitted tunneling probability function $T^{\mathrm{c}}_{\mathrm{fit}}$ (thick gray line in figure 4(a), where $c = 0.008$ nA V$^{-1}$). The obtained $(\mathrm{d}I/\mathrm{d}V)/T^{\mathrm{c}}_{\mathrm{fit}}$ curve successfully recovers the molecular surface-state peaks (see figure 4(b)). Although in our previous studies the $\mathrm{d}I/\mathrm{d}V$ curve measured on single $H_2Pc$ molecules could not resolve such molecular states in detail even using a lock-in amplifier [5, 7], in this study, because of the improved S/N of the tunneling current as well as the use of $T^{\mathrm{c}}_{\mathrm{fit}}$ normalization, six LDOS peaks (Gaussian fitting) below and above the Fermi energy are confirmed, corresponding to HOMO states at $-0.21$, $-0.38$, and $-0.93$ eV, and LUMO states at $+0.27$, $+0.54$, and $+1.21$ eV.

On the same sample surface, we investigated how the parameters in $T^+$ and $T^-$ affect the normalization. If $T^{\mathrm{c}}_{\mathrm{fit}}$ is too sensitive to the fitting parameters, slight changes in the parameters, such as, $\phi$ and $z$, can markedly change $T$, causing different LDOS peaks to be recovered. Thus, we obtained $T^{\mathrm{c}}_{\mathrm{fit}}$ with different work functions ($\phi$ of 3.5, 4.0, 4.5, and 5.0 eV) as well as with different tip–sample separations ($z$ of 10 and 11 Å), then normalized the $\mathrm{d}I/\mathrm{d}V$ curve in figure 4(a). Figures 4(c) and (d) show the obtained $(\mathrm{d}I/\mathrm{d}V)/T^{\mathrm{c}}_{\mathrm{fit}}$ curves. In spite of using different fitting parameters, the $(\mathrm{d}I/\mathrm{d}V)/T^{\mathrm{c}}_{\mathrm{fit}}$ curves are almost identical. In particular, the peak energy positions marked by dotted lines are exactly the same, i.e., slight differences in the parameters do not significantly

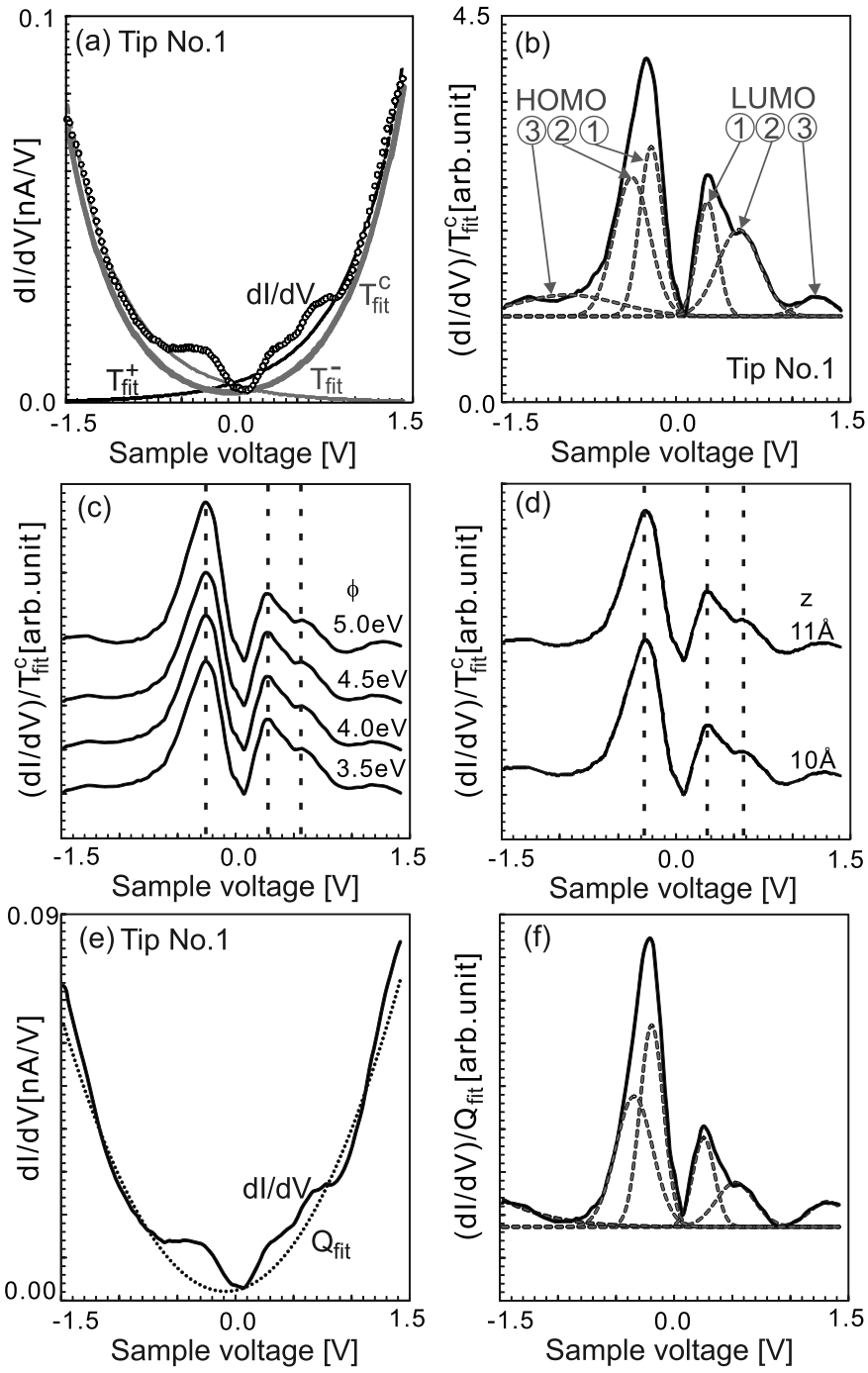


**Figure 4.** Tunneling spectroscopy measurements on a first $H_2Pc$ layer on Cu(111) were performed with a tip condition of No. 1. (a) An experimentally obtained $dI/dV$ curve (open circles) with a tip condition of No. 1 at $R = 2 \times 10^{10}$ Ω was fitted by $T_{fit}^{+}$ and $T_{fit}^{-}$, then normalized by $T_{fit}^{c}$ and the LDOS was recovered as shown in (b). In (b), a fit with Gaussian functions showed six LDOS peaks, which are named HOMO (1)–(3) for a negative voltage side, and LUMO (1)–(3) for a positive voltage side. (c) and (d) exhibit $(dI/dV)/T_{fit}^{c}$ curves normalized with different averaged barrier heights ($\phi$) of 3.5, 4.0, 4.5, and 5.0 eV in (c) and with different tip–sample separations ($z$) of 10 and 11 Å in (d). (e) The same $dI/dV$ curve in (a) (solid line) and its fitted quadratic function ($Q_{fit}$, dotted line). (f) A normalized $(dI/dV)/Q_{fit}$ curve obtained with $dI/dV$ and $Q_{fit}$ in (e).

affect the recovered LDOS. From an experimental view point, this is very convenient since we do not need to pay close attention when selecting the values of $\phi$ and $z$.

Since the tunneling probability function is exponential, we can also approximately normalize the $dI/dV$ curve using the quadratic function $Q(V) = aV^2 + bV + c$ where $a$, $b$, and $c$ are fitting parameters.

$$(dI/dV)/Q(V)_{fit} \propto \text{LDOS} \qquad (|V_S| < 1V), \tag{8}$$

$$Q(V)_{fit} = aV^2 + bV + c. \tag{9}$$

The $dI/dV$ curve in figure 4(a) was also normalized by its fitted quadratic function, as shown in figure 4(e).

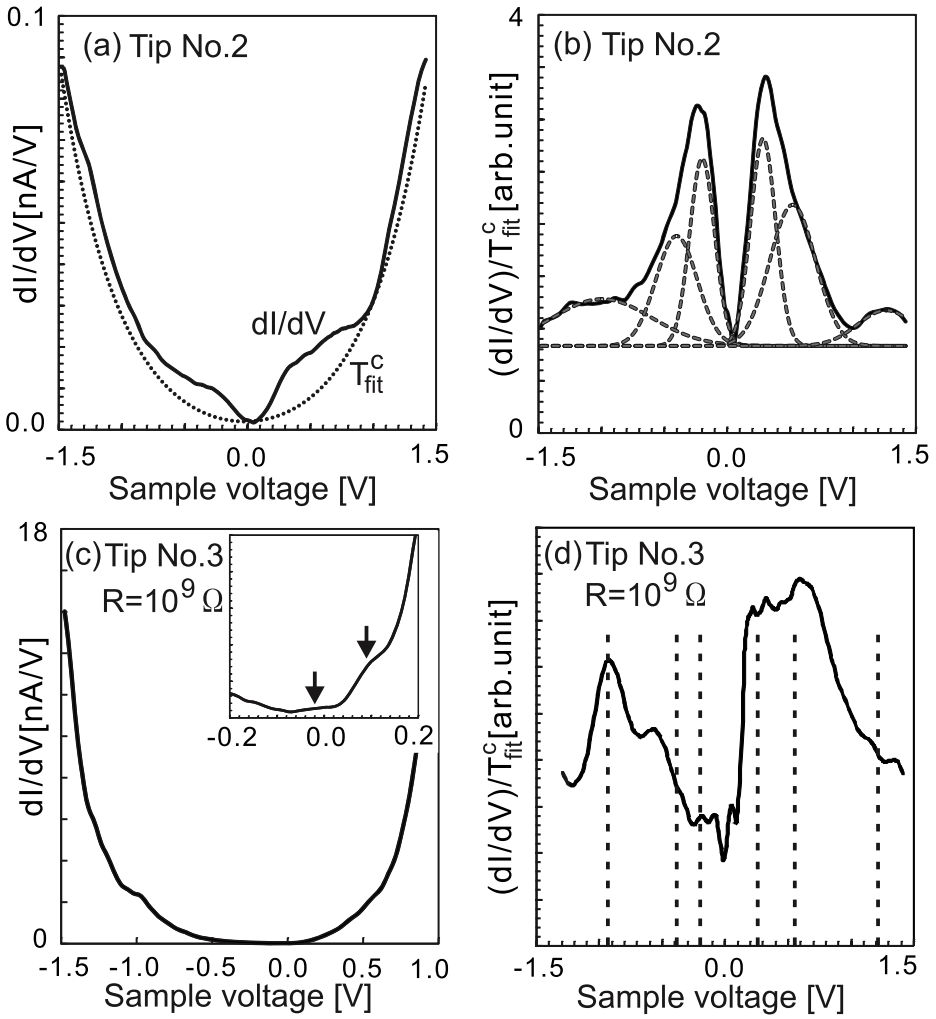


**Figure 5.** Tunneling spectroscopy measurements on a first $H_2Pc$ layer on Cu(111). (a), (b) and (c), (d) were obtained with different tip conditions of No. 2 and No. 3, respectively. (a) An experimentally obtained $dI/dV$ curve (solid line) at $R = 2 \times 10^{10}$ Ω with a tip condition of No. 2 and fitted $T^{c}_{fit}$. (b) A normalized $(dI/dV)/T^{c}_{fit}$ curve obtained with $dI/dV$ and $T^{c}_{fit}$ in (a). (c) An experimentally obtained $dI/dV$ curve with a tip condition of No. 3 at $R = 3 \times 10^{9}$ Ω. The inset shows an enlarged $dI/dV$ curve near the Fermi energy. (d) $(dI/dV)/T^{c}_{fit}$ curve obtained with the $dI/dV$ in (c).

**Table 1.** Energy positions of LDOS (HOMO&LUMO) peaks of $H_2Pc$ on Cu(111).

| | HOMO(1) (eV) | HOMO(2) (eV) | HOMO(3) (eV) | LUMO(1) (eV) | LUMO(2) (eV) | LUMO(3) (eV) |
|---|---|---|---|---|---|---|
| $(dI/dV)/T^{c}_{fit}$, tip No. 1 | −0.21 | −0.38 | −0.93 | +0.27 | +0.54 | +1.21 |
| $(dI/dV)/Q_{fit}$, tip No. 1 | −0.19 | −0.34 | −3.00 | +0.25 | +0.53 | +1.32 |
| $(dI/dV)/T^{c}_{fit}$, tip No. 2 | −0.20 | −0.40 | −0.99 | +0.28 | +0.52 | +1.26 |
| $(dI/dV)/T^{c}_{fit}$, 1D chain | −0.22 | −0.45 | −0.98 | +0.33 | +0.83 | |
| $(dI/dV)/T^{c}_{fit}$, single molecule | −0.17 | −0.34 | −0.78 | +0.26 | +0.48 | +1.18 |

The $(dI/dV)/Q_{fit}$ curve show LDOS peaks (figure 4(f)) corresponding to HOMO states at −0.19, −0.34, and −3.00 eV, and LUMO states at +0.25, +0.53, and +1.32 eV. Comparing these peak positions with the peaks in figure 4(b) (see table 1), we found that HOMO(1), HOMO(2), LUMO(1), and LUMO(2) are almost the same, while HOMO(3) and LUMO(3) are shifted by more than 100 meV. This indicates that $Q$ normalization is effective for recovering LDOS peaks within ±1 eV around the Fermi energy. This $Q$ normalization is particularly useful when the $dI/dV$ curve can only be measured within ±1 eV, for example, in the case that unstable molecules start to move upon the application of a sample voltage above ±1 V.

$dI/dV$ curves vary slightly even when measured on the same sample area using the same tip. This is caused by a slight change in the atomic structure at the tip apex during the scanning owing to the high electric field between the tip and sample, or molecules or atoms adhering to the apex. This variation slightly changes the tip work function, leading to different $T$ and $dI/dV$ curves. Figures 5(a) and (b) were

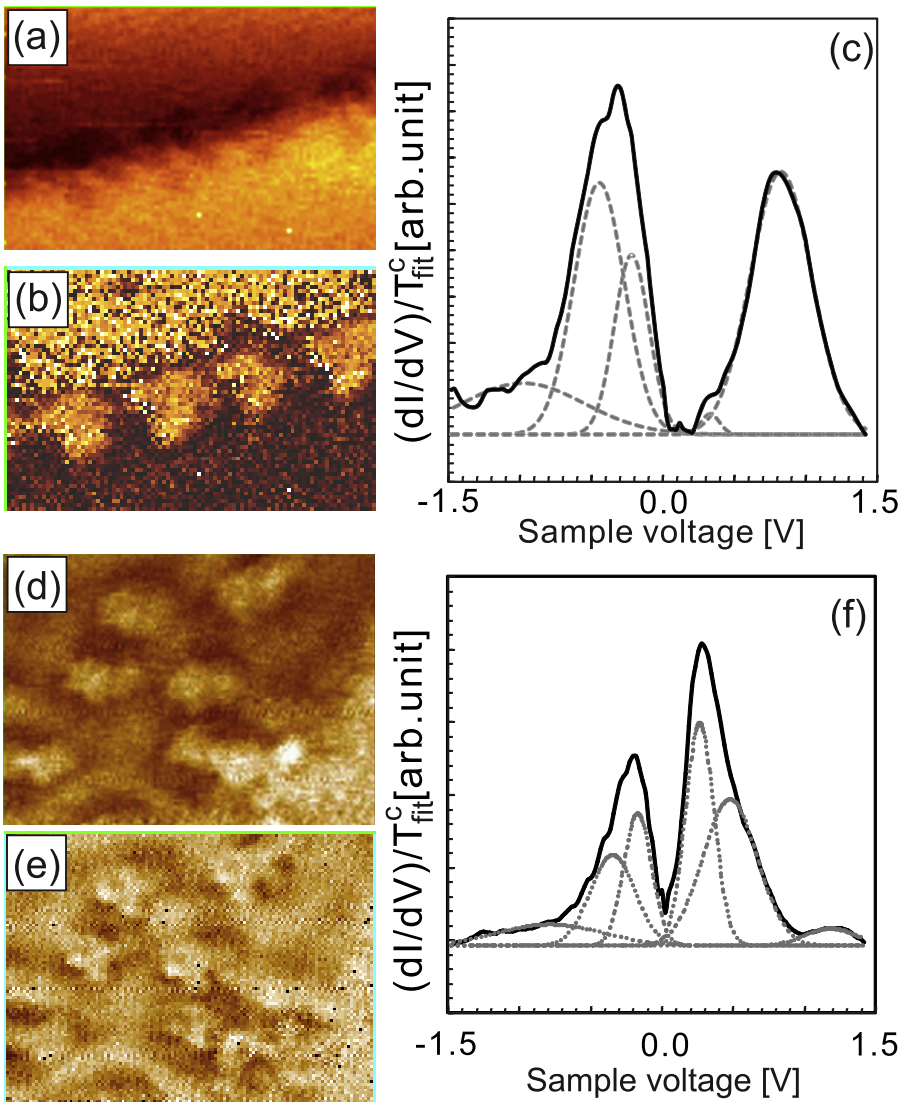


**Figure 6.** (a)–(c) STM/STS measurements of a one-dimensional $H_2Pc$ molecular chain at the edge of a 1 ML molecular island. (a) An STM topographic image ($7.5 \times 4.9$ nm$^2$, $V_s = -1.5$ V, $I = 100$ pA). (b) A $dI/dV$ map at $+0.75$ V obtained at the same area as (a). (c) A $(dI/dV)/T^c_{fit}$ curve (solid line), corresponding to LDOS, obtained at a single-molecular one-dimensional chain and fitted Gaussian functions (gray dotted lines). (d)–(f) STM/STS measurements of single $H_2Pc$ molecules on a first $H_2Pc$ molecular layer. (d) An STM topographic image ($10 \times 7$ nm$^2$, $V_s = -1.5$ V, $I = 100$ pA). (e) An $I(V)$ map at $-1.4$ V obtained at the same area as (d). (f) A $(dI/dV)/T^c_{fit}$ curve (solid line), corresponding to LDOS, obtained at single molecules and fitted Gaussian functions (gray dotted lines).

obtained at exactly the same area as figure 4(a). Only a slight change in the tip apex during scanning results in a different $dI/dV$ curve (we named this tip condition 'Tip No. 2'). We normalized this $dI/dV$ curve (solid line in figure 5(a)) using its $T^c_{fit}$ (dotted line in figure 5(a)). Since the sample LDOS is independent of the tip condition even when $dI/dV$ curves have different shapes, we recovered the identical LDOS peaks as figure 4(b). The $(dI/dV)/T^c_{fit}$ curve in figure 5(b) has six LDOS peaks corresponding to HOMO states at $-0.20$, $-0.40$, and $-0.99$ eV, and LUMO states at $+0.28$, $+0.52$, and $+1.26$ eV. Comparing these peak energy positions with those in figure 4(b) (see table 1), all peaks are identical within 60 meV. This proves that $T^c_{fit}$ normalization can reproducibly recover the LDOS peaks.

Table 1 shows that $T^c_{fit}$ normalization as well as $Q_{fit}$ normalization can recover the LDOS peaks with a high accuracy, particularly HOMO/LUMO states near the Fermi energy ($\pm 1$ eV). Although from figures 1(c) and (d) we concluded that there was a strong tip–sample interaction at $R = 1 \times 10^9$ Ω, we evaluated how $dI/dV$ measurement is affected by the interaction. Figures 5(c) and (d) were obtained on the same sample area after obtaining figures 4(a)–(f) and 5(a), (b). The strong tip–sample interaction causes instability in nanomolecules, which frequently causes spike-like noises in the tunneling current, disturbing the $dI/dV$ measurement. Despite this, after several trials, we were able to obtain the $dI/dV$ curve shown in figure 5(c). (However, we observed some changes on the molecular surfaces after the spectroscopy measurements.) At $R = 1 \times 10^9$ Ω, the tip–sample separation is smaller than that in the case shown in figure 4(a), which markedly increases the $T$ background (the $dI/dV$ value at $-1.5$ V increases to $\sim$15 nA V$^{-1}$). The $dI/dV$ curve in figure 5(c) appears to be an exponential function without any features of the molecular density of states (no

clear peaks, shoulders, or bumps near the Fermi energy). Without careful checking, it might be concluded that a gap exists around the Fermi energy, but careful examination of the d$I$/d$V$ curve around the Fermi energy (see the enlarged d$I$/d$V$ curve in figure 5(c)) reveals small features (bumps and shoulders), i.e., at $R = 10^9$ Ω, a large $T$ can bury the signal of a weak molecular LDOS.

Frequently, a lock-in amplifier is used to obtain d$I$/d$V$ curves. However, such a d$I$/d$V$ signal is dimensionless. Therefore, when a flat d$I$/d$V$ signal is experimentally obtained around the Fermi energy, it is difficult to distinguish between a gap and a buried LDOS peak in the $T$ background. To avoid misinterpretation, it is advisable to verify the d$I$/d$V$ curve by numerical differentiation of the $I(V)$ curve to determine whether d$I$/d$V$ is zero at $V_S = 0$.

The d$I$/d$V$ curve in figure 5(c) was normalized by $T^c_{fit}$. The obtained (d$I$/d$V$)/$T^c_{fit}$ curve recovers LDOS as shown in figure 5(d). Dotted lines in figure 5(d) show LDOS peak positions in figure 4(b), which mostly fit the peak and shoulder positions in figure 5(d). This also proves that $T^c_{fit}$ normalization is a very powerful technique for recovering LDOS peaks.

Using $T^c_{fit}$ normalization, we studied the molecular electronic states of 1D molecular chains and single molecules. Figure 6(a) shows an STM topographic image around the edge of a 1 ML molecular island on Cu(111), where single molecules form 1D chains. In the topographic image (figure 6(a)), it is difficult to observe the molecular chains, but a d$I$/d$V$ map at +0.75 V clearly shows the molecular chains (figure 6(b)). The obtained d$I$/d$V$ curves were normalized using $T^c_{fit}$ and the LDOS peaks corresponding to HOMO states at −0.22, −0.45, and −0.98 eV, and LUMO states at +0.33 and +0.83 eV (see figure 6(c) and table 1) were recovered. The molecular chains have the same HOMO states as the film, but the LUMO states are shifted to +0.83 eV with a small peak at +0.33 eV.

The LDOS peaks of single molecules on the first $H_2Pc$ layer were also measured. Figures 6(d) and (e) show a topographic image and an $I(V)$ map taken at −1.4 V, respectively. Bright dots correspond to the single molecules. Figure 6(f) shows the recovered LDOS peaks which correspond to HOMO states at −0.17, −0.34, and −0.78 eV, and LUMO states at +0.26, +0.48, and +1.18 eV (see table 1). Single molecules on the first $H_2Pc$ layer were confirmed to have the same LDOS as the first $H_2Pc$ layer (figure 4(b)).

## 4. Conclusions

We demonstrated a technique for recovering the molecular LDOS from d$I$/d$V$ curves experimentally obtained by scanning tunneling spectroscopy (STS) on low-dimensional phthalocyanine ($H_2Pc$) nanomolecules on a clean and atomically flat Cu(111) substrate. Owing to the weak bonding between the molecules and the noble metal surface, and to avoid the tip–sample interaction in tunneling spectroscopy, a large tip–sample separation is required, which necessitates low-noise measurements and the hiding of LDOS signals. $T^c_{fit}$ normalization successfully recovered the molecular LDOS from the d$I$/d$V$ curves taken at a large $T$. $Q_{fit}$ normalization was also very effective in recovering the LDOS within ±1 eV near the Fermi energy. Slight differences in fitting parameters did not significantly affect the recovered LDOS. LDOS peaks were observed below (−) and above (+) the Fermi level at −0.21, −0.38, −0.93, +0.27, +0.54, and +1.21 eV on the first $H_2Pc$ layer, and at −0.22, −0.45, −0.98, +0.33, and +0.83 eV on 1D $H_2Pc$ chain molecules. Single $H_2Pc$ molecules had LDOS peaks at −0.17, −0.34, −0.78, +0.26, +0.48, and +1.18 eV, whose energy positions are very close to that on the first $H_2Pc$ layer.

## Acknowledgments

We thank Professor Dr H Ishii, Dr F Shibahara, and Dr Y Noguchi for assistance in the purification of our molecules. The low-current-noise was realized with the support of Professor Dr W Wulfhekel as well as the technical support of Dr T Schuh. Vacuum conditions in our STM setups have been improved by the support of Dr T Uchihashi, Professor Dr I Arakawa, and Mr Y Shimokawa. We thank Mr N Bachellier for carefully reading our manuscript. This work was supported by JSPS KAKENHI Grant Numbers 22810005, 23681018, Japan Science and Technology Agency (JST)—Improvement of Research Environment for Young Researchers: Chiba University Young Research-Oriented Faculty Member Development Program in Bioscience Areas, Chiba University Global COE Program: Advanced School for Organic Electronics, Casio Science Promotion Foundation, Asahi Glass Foundation, Hatakeyama Culture Foundation, The Association for the Progress of New Chemistry, Iketani Science and Technology Foundation, The Noguchi Institute, Ozawa Yoshikawa Memorial Electronics Foundation, Research Foundation for the Electrotechnology of Chubu, The Nakajima Foundation, The Futaba Electronics Memorial Foundation, and Shimadzu Foundation.

## References

[1] Walter M G, Rudine A B and Wamser C C 2010 *J. Porphyrins Phthalocyanines* **14** 759
[2] Nothaft M, Hohla S, Jelezko F, Fruhauf N, Pflaum J and Wrachtrup J 2012 *Nature Commun.* **3** 628
[3] Jackson T N 1998 *IEEE J. Sel. Top. Quantum Electron.* **4** 100
[4] Tang C W, VanSlyke S A and Chen C H 1989 *J. Appl. Phys.* **65** 3610
[5] Schmaus S, Bagrets A, Nahas Y, Yamada T K, Bork A, Evers F and Wulfhekel W 2011 *Nature Nanotechnol.* **6** 185
[6] Bagrets A, Schmaus S, Jaafar A, Kramczynski D, Yamada T K, Alouani M, Wulfhekel W and Evers F 2012 *Nano Lett.* **12** 5131
[7] Takacs A F, Witt F, Schmaus S, Balashov T, Bowen M, Beaurepaire E and Wulfhekel W 2008 *Phys. Rev.* B **78** 233404
[8] Brede J, Atodiresei N, Kuck S, Lazic P, Caciuc V, Morikawa Y, Hoffmann G, Blügel S and Wiesendanger R 2010 *Phys. Rev. Lett.* **105** 047204
[9] Miyamachi T *et al* 2012 *Nature Commun.* **3** 938
[10] Komeda T, Isshiki H, Liu J, Zhang Y F, Lorente N, Katoh K, Breedlove B K and Yamashita M 2010 *Nature Commun.* **2** 217

[11] Mugarza A, Robles R, Krull C, Korytar R, Lorente N and Gambardella P 2012 *Phys. Rev.* B **85** 155437
[12] Tanaka Y, Mishra P, Tateishi R, Cuong N T, Orita H, Otani M, Nakayama T, Uchihashi T and Sakamoto K 2013 *ACS Nano* **7** 1317
[13] Zhao A *et al* 2005 *Science* **309** 1542
[14] Tsukahara N *et al* 2009 *Phys. Rev. Lett.* **102** 167203
[15] Gerhard L, Yamada T K, Balashov T, Takacs A F, Daena M, Ostanin S, Ernst A, Mertig I and Wulfhekel W 2010 *Nature Nanotechnol.* **5** 792
[16] Ukraintsev V A 1996 *Phys. Rev.* B **53** 11176
[17] Yamada T K, Bischoff M M J, Mizoguchi T and van Kempen H 2002 *Surf. Sci.* **516** 179
[18] Yamada T K, Bischoff M M J, Heijnen G M M, Mizoguchi T and van Kempen H 2003 *Phys. Rev. Lett.* **90** 056803
[19] Kuk Y and Silverman P J 1990 *J. Vac. Sci. Technol.* A **8** 189
[20] Sanchez O, Garcia J M, Segovia P, Alvarez J, Vazquez de Parga A L, Ortega J E, Prietsch M and Miranda R 1995 *Phys. Rev.* B **52** 7894
[21] Nicolay G, Reinert F, Hufner S and Blaha P 2001 *Phys. Rev.* B **65** 033407
[22] Stroscio J A, Pierce D T, Davies A, Celotta R J and Weinert M 1995 *Phys. Rev. Lett.* **75** 2960
[23] Bischoff M M J, Yamada T K, Fang C M, de Groot R A and van Kempen H 2003 *Phys. Rev.* B **68** 045422
[24] Okuno S N, Kishi T and Tanaka K 2002 *Phys. Rev. Lett.* **88** 066803
[25] Kleiber M, Bode M, Ravlic R and Wiesendanger R 2000 *Phys. Rev. Lett.* **85** 4606